Hydrogen in Strong DC and Low Frequency Electric Fields – One Dimensional Atoms

M.H. Nayfeh, D. Humm, and M. Peercy

Department of Physics, University of Illinois at Urbana-Champaign,
1110 West Green Street, Urbana, IL61801, USA

Introduction

Recently there has been a resurgence of interest in the effects of externally applied electric, magnetic, and radiation fields upon atomic spectra and collision processes, due to the development of the ability to produce, in the laboratory, fields which are comparable in strength to internal atomic fields[1-3]. But it is almost impossible to create fields in the laboratory (10^9 V/cm) which are strong enough to disrupt atoms in their normal states. On the other hand, a Rydberg atom, which can be thousands of angstroms in size, is very sensitive to external perturbations, and the Coulomb field of the nucleus can be overcome by an external electric field of only 5 kV/cm. Thus entry of atomic physics into the strong-field regime has been accomplished by dealing with highly excited states, rather than by generating enormous laboratory fields. Diverse strong field effects are now studied in the laboratory under easily controlled conditions. These studies have extended the scope of research in areas which once used only weak field effects, and they have also opened up new avenues.

The treatment of the problem is not straightforward because of the different symmetries involved and because the Rydberg electron does penetrate the core; thus the many-particle nature cannot be avoided. A strong candidate for a unified treatment of Rydberg atoms in fields is the frame transformation approach.[4] Its basic idea is that configuration space can be separated into two regions where different dynamics prevail: an inner region, where the Rydberg electron penetrates the ionic core, and where the many-particle nature of the system must be considered; and an outer region, where the interaction between the Rydberg electron and the residual ion can be adequately represented by long-range potentials. The equations of motion are solved separately in each region and matched to a common boundary condition. This approach has been extensively developed in field-free atomic physics, under the general heading of R-matrix and quantum defect methods. It offers the possibility for dealing with the interplay between effects of particular atomic structures and of electron motion in Coulomb plus external fields, since these are associated respectively with inner and outer region dynamics.

An important implication of this point of view is that the physics of highly excited atoms in external fields should be described in terms of hydrogen, and that specific knowledge of the behavior of atomic hydrogen in external fields should provide the key to general understanding. In fact, theory has tended to focus almost exclusively on hydrogen. Because applications to complex atoms have been in mind, these calculations focused on excitation from spherical low-lying states of good orbital angular momentum. But under these field values this "hydrogenic theory" does not really apply to hydrogen itself. This is due to the fact that the Stark splitting at these fields are larger than the Lamb shifts, fine and hyperfine splittings for all levels of hydrogen including n=2 for which these are the largest.

The Hydrogen Atom Editors: G.F. Bassani · M. Inguscio · T.W. Hänsch

Thus as a result of the near ℓ degeneracy, the field mixes fully the ℓ quantum numbers, causing ℓ not to be a good quantum number and the states become pure parabolic with permanent dipole moments.

Our experimental and theoretical work has indeed shown that hydrogen in strong electric fields is unique among all atoms even in the energy region close to E = 0 where complex atoms are believed to become practically hydrogenic. In fact hydrogen in strong electric fields offers the only atomic system of combined true spherical symmetry (non-relativistic interaction) and cylindrical symmetry (dc field).

One of the novel features of the combined pure symmetries is the ability to drastically manipulate and even design and construct specific atomic structures.[5-6] Although the first generation of experiments used alkali and earth alkali and metastable excited rare gas atoms because their excitation is within the reach of the visible tunable dye lasers,[1,7-10] however, it was soon realized that the noncoulombic interaction with the ion core in complex atoms hampers one's control of the manipulation and design. Therefore the attention turned to atomic hydrogen in spite of the fact that it is not readily amenable to experimentation.[11-12] However this difficulty is offset by much theoretical interest in this system.[13-16]

In our studies, we use strong external dc electric fields to manipulate and control the atomic structure of highly excited atomic hydrogen. We can construct nearly one-dimensional atoms whose electronic distribution are highly extended along the field, and which may have enormous dipole moments ("giant dipole" atoms).[17-18] The nuclear charge Z_1 that defines the energy and other properties of the "new" atom is a fraction of the proton charge. We can construct orbits that are aligned (m = 0) or at an angle (m ≠ 0) with the field. For m = 0, the fractions 0, 1/4, 1/2, 3/4 and 1 define four quarters that classify the atoms.[18] The dipole moment is found to be opposite to the field in the first and third, and in its direction in the second and fourth quarters, and zero at the boundaries. For |m| = 1, on the other hand, only the fractional charges, 0, 1/2, and 1 are of importance; they give two halves that classify the atoms with the dipole moment being in the direction and opposite to the field in the first and second halves respectively.[18]

These one-dimensional atoms can be prepared with total positive or negative energy. Although these are unstable against ionization, however at E < 0 F but E > -2 $\sqrt{F}$ one can populate "giant dipole" atoms whose potential barriers are large enough (tunneling small enough) to render their lifetimes quite long, important for further experimentation and application.

Another unconventional property of these one-dimensional atoms is their radiative interaction with strong fields (EP of low frequency ω).[19] Their huge permanent electric dipole moment d couples very strongly to the oscillating field, dressing the atom frequency modulations and producing sidebands with spacing ω and whose strength is governed by dE/ω. A red one of these bodies can then interact near resonantly with the oscillating field effectively inducing transitions between the original undressed levels. Moreover our analysis indicates that as the excitations proceed from an initial state, the dressing might become strong enough at higher levels to cause the off ladder transitions to become comparable in strength to the ladder transitions causing a loss of the one-dimensionality.

Experimental Technique

Recently, a number of schemes have been employed for the preparation of highly excited atomic hydrogen.[11,20-22] Here simultaneous absorption of two photons from a single tunable pulsed laser beam at 243 nm results in excitation from 1s to n-2, and some photoionization of the resulting n=2 population. A second pulsed beam excites states near the continuum from the n=2 states as shown in Fig. 1. For properly chosen 243 nm energy densities, a large population at n=2 atoms can be produced with only a few percent of them being photoionized. The second beam is then capable of promoting a large portion of the remaining excited atoms to a well-defined high-lying state without saturating the process. Previously the two photon Doppler-free spectroscopy of the n=2 state has been performed using radiation at 243 nm; however, no attempt to excite the hydrogen atoms further was reported.[25]

Figure 2 shows a block diagram of the experimental setup.[12] The atomic hydrogen source is a modified Wood discharge tube. An atomic beam is formed by effusion from the discharge region through a multicollimator assembly composed of 25 small glass capillaries. The thin-walled capillaries are 4 mm long, with an inside diameter of about .2 mm. The resulting atomic beam is directed into the diffusion pumped cell which contains the field plates. The beam is loosely collimated, but produces a density of about 10^{11} H°/cm^3; the background gas density is on the order of 10^{12}/cm^3. One of the plates has a 3 mm × 10 mm slot cut into it to allow the passage of ions. Since the presence of the open slot would lead to an unacceptably non-uniform field, a .5 mm spacing copper mesh was soldered over the whole surface of the plate. The electric field between the plates is determined to an accuracy of 0.5% by measurement of the applied voltage and the separation of the field plates. Ions produced by the laser radiations are driven by the electric field through the slot in the grounded plate. They travel through a 100 cm long, field-free drift tube which provides mass analysis. This is necessary since molecular impurities are easily ionized by the ultra-violet wavelengths in use. At low electric fields, the mass resolution is sufficient to verify that the signal under study is indeed due to atomic hydrogen.

Fig. 1

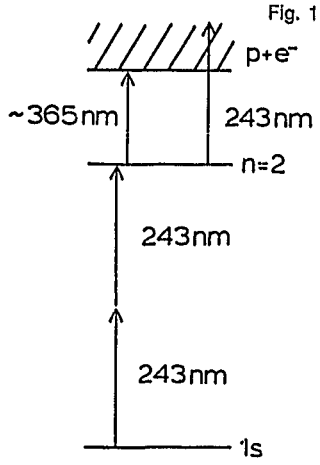

Fig. 2

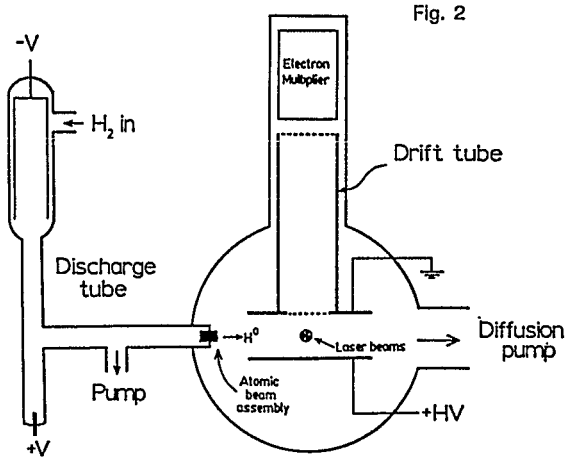

Fig. 1 Excitation of highly excited states of atomic hydrogen. Absorption of two photons each at 2430 Å excites the ground state to 2s followed by one photon excitation at 3660 Å to a highly excited state.

Fig. 2 A simplified block diagram of the experimental set up.

The resolution at kilovolt/cm range fields is sufficient to separate the hydrogen signal from those due to the impurities. Ions are detected using an 18 stage venetian blind electron multiplier capable of single ion detection. Under typical experimental conditions, several hundred ions are detected per pulse.

The transit time t_s of thermal hydrogen across the effective observation region (1.5 mm - half of the width of the slot in the upper plate) will cutout the ionization produced by states that ionize very slowly such that $\tau >> t_s$ where τ is the ionization lifetime of the atom. On the other hand, ionization from states that ionize in time much shorter than t_s will not effectively be affected by the slot. For intermediate cases, the detection factor is just $1-e^{-t_s/\tau}$. Using 1.5×10^3 m/s for the thermal velocity of hydrogen in the direction parallel to the width of the slot gives 10^{-6} s for t_s.

The optical beams needed for the excitation of atomic hydrogen are produced using a pulsed laser system: an Nd^{+3}:YAG laser and two dye lasers. A fraction of the second harmonic of the YAG laser at 532 nm is used to pump one of the dye lasers producing a beam at 630 nm, which is frequency doubled to 315 nm by a KDP crystal and then summed with the residual YAG fundamental by a KDP crystal resulting in a beam at 243 nm of pulse length of about 10 ns, a bandwidth of about 1.5 cm^{-1} and pulse energies on the order of 10 microjoules. The second dye laser produces a beam at about 555 nm which is summed with part of the YAG fundamental to produce a beam with pulse length near 10 ns, bandwidth of .8 cm^{-1}, pulse energies of a few tenths of a millijoule and a wavelength near 365 nm. The data are collected and analyzed using an LSI-11 computer system.

Thus, for this test both field plates were grounded until one microsecond after the passage of the laser pulses. At this time a high voltage pulse resulting in a 1 kV/cm field between the plates was applied, thereby field-ionizing the highly excited atoms and collecting the ions. Figure 3 shows the results of averaging 8 scans of the ionization in the region of some high Rydberg states.[23,24] Resonances are seen corresponding to the excitation of states up to about 60p. The loss of the series at

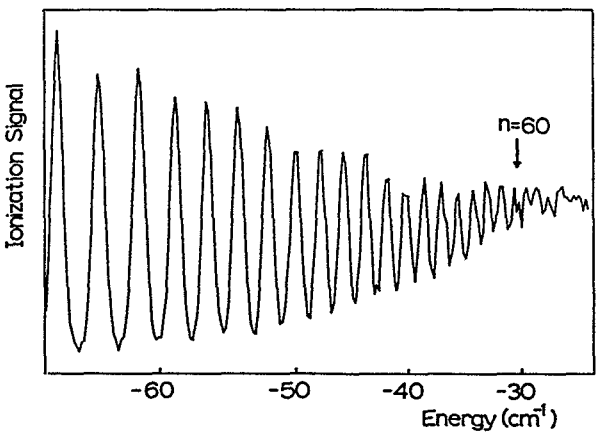

Fig. 3 Highly excited hydrogen spectrum produced by pulsing the electric field after the excitation which lasts 10ns has taken place. The loss of resolution beyond n = 66 is due to the fairly wide bandwidth of the 3660 Å laser (1 cm^{-1}).

this principle quantum number indicates an instrumental resolution of about 1 cm^{-1}, due mostly to the laser linewidth and some residual Doppler broadening (.1 cm^{-1}) due to the relatively large angular spread of the dense atomic beam.

2. Effect of field on n = 2

We first discuss the effect of the electric field on the n = 2 state, the lowest excited state.[26] For one reason, the response of this state is known and allows us to discuss the weak and intermediate field limit. More importantly, this state acts as an intermediate resonance state in our excitation of the highly excited states and therefore it is necessary to understand its structure. Since we are interested in applying fields larger than 2 kV/cm, we will not include the Lamb shift in our analysis. In the region of 2-5 kV/cm, only n and m_j are good quantum numbers, but neither j and ℓ, nor the parabolic quantum numbers (n_1, n_2, m) are. At fields higher than 5 kV/cm, the interaction with the Stark field dominates over the fine structure, thus leading to a linear Stark splitting; consequently, the states can have good parabolic quantum numbers: the state (1,0,0) originating from $p_{3/2}$ is what we call the m=0 blue state, whereas the state (0,1,0) originating from $p_{1/2}$, $s_{1/2}$ is what we call the m=0 red state. The |m|=1 state is the least shifted state. Such calculations were previously done for n=2, 3, and 4.[27] Numerical results based on these calculations are given in Fig. 4.

We will now discuss the efficiency of populating the various Stark states of n=2 using the two-photon (π polarization) process. We calculated the percentage of population of the |m|=1,m=0 blue state and m=0 red state as a function of the electric field (F ≥ 2 kV/cm) assuming the states are not resolved. It is known that in the zero field limit |m|=1 state is not excited in the π-π excitation. The presence of a field of 3 kV/cm produces about 30%, however, at high fields (> 10 kV/cm) this population drops to less than a few percent. We also note that the two m=0 states approach 50 percent populations at higher fields with the red one approaching this value faster than the blue one.

We calculated the percentage of purity of the various states if each state is selectively excited by radiation whose effective bandwidth is less than the splittings (those are shown in Fig. 5). Above 10 kV/cm both of the m=0 states can be purely excited (> 97%) whereas the |m| =1 state is not excitable. But, because our laser bandwidth is ~1.5 cm^{-1}, then in practice we can only excite pure parabolic states using fields larger than 10 kV/cm such that the Stark splitting is larger than 3 cm^{-1}. Since we use quite low atomic hydrogen density, we find no problem in dropping up to 18 kV/cm across our interaction region; thus making these kinds of studies feasible.

Figure 6 gives the charge distribution of the 100, 010, and 001 parabolic states of n=2. The figure shows the x-z cross section through the atom with the nucleus being at the center of the system. The curves are lines of constant charge density ($\rho = \psi\psi^* =$ constant) where the total charge is normalized to unity. The large eccentricity in the charge distribution of the m_ℓ=0 blue and red states is quite evident, the concentration being up and down field respectively. On the other hand, the distribution of the image 001 state is symmetric with respect to the field. This figure also shows that the charge distribution of the red and blue states are mirror images of each other when reflected in the z = 0 plane. This property is utilized in the present study as a means of probing the shape of the electronic distributions of highly excited Stark states.

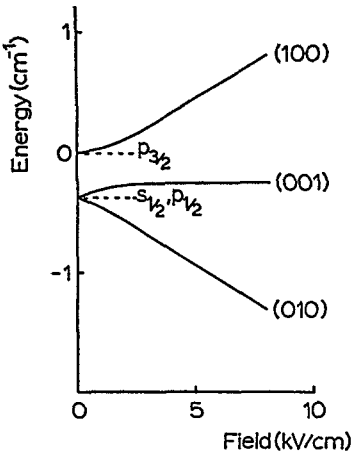

Fig. 4

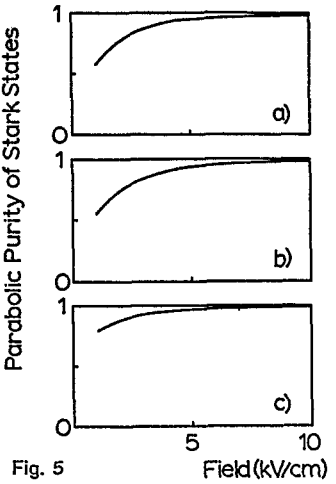

Fig. 5

Fig. 4 The splitting of the n = 2 states vs. field including the effects of the fine structure (but ignoring the Lamb shift). The Stark states are labeled at high field by the parabolic states to which they tend.

Fig. 5 Purity of the Stark states vs. field in terms of their high-field limit parabolic states, (a) is for the blue-shifted 100 state, (b) is for the unshifted 001 state, and (c) is for the red-shifted 010 state.

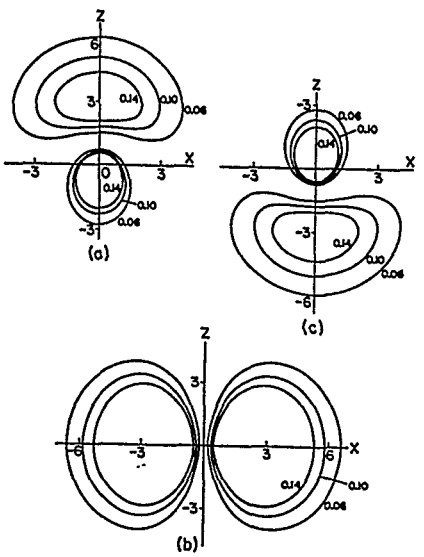

Fig. 6 Charge distribution of the parabolic states of n = 2 state of hydrogen, (a) is for the blue-shifted (1,0,0) state, (b) is for the unshifted (0,0,1) state, and (c) is for the red-shifted (0,1,0) state.

3. Effect of dc field on highly excited hydrogen--Atomic Engineering

Although the potentials represented using spherical coordinates in the z = 0 plane (shown in Fig. 7a) can be very useful in bringing out some features of the interaction, they are not very useful for quantitative calculation. This is because the nonspherical symmetry of the potential makes the interaction non-separable: that is, it cannot be separated into three independent one dimensional motions in spherical coordinates. The interaction, however, is separable in parabolic coordinates $\xi = r + z$, $\eta = r - z$, and ϕ the azimuthal angle, with quantum numbers n_1, n_2, and m respectively. The effective potentials for the ξ and η motions shown in Figs. 7 b,c in fact have good resemblance to that of the z cut in the $z < 0$ and $z > 0$ regions respectively, and hence govern the energy of the system (location of the energy) and the ionization lifetimes of these levels, respectively. The quantum number m is common to both parabolic and spherical descriptions, and the principle quantum number $n = n_1 + |m| + 1$. The spherical l and parabolic n_1, n_2 quantum numbers do not have a one-to-one correspondence: a state with definite values of n_1 and n_2 is composed of many different values of ℓ.

One important property of the atom that comes out of this procedure is the fact that only a fraction of the nuclear charge $Z_1 < 1$ drives the ξ motion and hence dictates the energy of the system, while the rest of the charge $Z_2 = 1 - Z_1$ drives the free η motion and hence dictates its lifetime. Thus the presence of an external electric field provides us with a situation where the nuclear charge that drives the bounded motion can be varied, in a near continuous fashion. Considering the fact that the physical and chemical identity of isolated atoms is defined by the nuclear charge, then it is clear that we have at our hand a means for creating new "types" of atoms.

We will now discuss the preparation and nature of the new types of atoms by discussing their spectroscopic properties such as ionization lifetimes, charge distributions (or excitation dipole moments), and branching ratios (or excitation strengths). To do so we will consider the positive and negative energy regimes separately, starting with the former.

Let us assume that atomic hydrogen is immersed in laser radiation of energy just larger than 13.6 eV, the ionization potential of hydrogen, and whose polarization is along the external dc electric field in

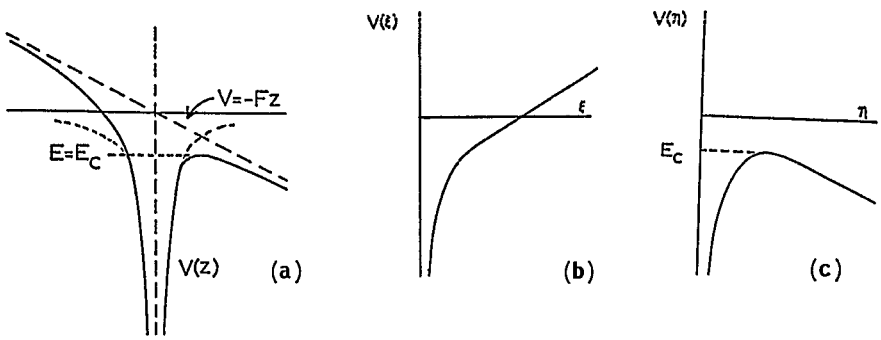

Fig. 7 Schematic of the potential of hydrogen in external dc electric. (a) Potential for a cut along the z axis in the presence of an electric field along the z axis showing a rise and a depression of the Coulomb potential in the $z \leq 0$ and $z \geq 0$ regions respectively. (b) and (c) are the same potential of (a) plotted as two one dimensional potentials in the $\xi = r + z$ and $\eta = r - z$ parabolic coordinates.

which the atom is immersed. Because of this choice of polarization, the electron gets an initial kick along the dc field, and the energy of the system is raised by 13.6 eV, thus rising to zero total energy. The electron can now execute bound motion even for this positive energy. The motion of the electron is nearly a one-dimensional motion with the orbit resembling a cigar whose axis is along the external field, the nucleus being located inside it near its lower tip (Fig. 8a). This specifically tailored atom lives on the order of 5×10^{-13}s (giving very broad widths), and the electron executes on the average about 5 rounds before it breaks away from the proton on its own, and it is found to spend most of its time away from the nucleus, near the upper tip of the cigar. If the electron were initially kicked perpendicular to the field (laser polarization perpendicular to the external field), the cigar would have been created at an angle with the field. (See Fig. 8b.).

The extraordinary thing about this cigar atom is that such a "separated charge" distribution gives a dipole moment P which points opposite to the external field. Moreover, the dipole is very large since the separation of the charge (length of the cigar) is about 1600 Å, hence giving dipole moments that are 3000 times larger than those of normal atoms. For this reason we call these atoms "giant dipole" atoms. However, in general, one cannot exclusively prepare these types of atoms without preparing the highly excited normal atom since, first of all, the excitation has to start from the ground state of the normal atom which is only weakly affected by electric fields and secondly both Coulomb and Stark fields will have to compete. Therefore, after the excitation process we always have a superposition of these two types with the branching ratio depending on a number of parameters including the total energy of the system, field strength, and the properties of the exciting laser radiation.[13-17] For example, the "visibility" of the giant dipoles, which is a measure of how much they rise above the accumulated smooth continuum, tends to be very small (4% at 5 kV/cm). This visibility gets worse at higher energy because these states get closer to each other in energy as the potential opens up. Those states were first seen in complex atoms such as rubidium, sodium, barium, krypton, and yttrium during 1978-1983,[1,7-10] but were found to have strengths that are smaller than is predicted for hydrogen. Theories that included the effect of core electrons explained the reduction of the strength.[15] The first observation of the giant dipoles in hydrogen was made in 1984 in our laboratory at the University of Illinois[12] (see Fig. 9). Similar observation was also achieved at the University of Bielefeld.[11]

Considering the shortness of their lifetimes, and the low efficiency of excitation, it is clear that experimentation with these "new atoms" will not be easy unless these two properties are enhanced. Recently we have been able to improve the efficiency[26] and to produce giant dipoles that live much longer than 10^{-12} s[18,19] in atomic hydrogen. We will discuss the efficiency first. The scheme we devised for this purpose relies on a process we call multistage shaping or charge shape tuning of the charge of the atom. In one-photon excitation from the ground state one effectively starts from a spherically symmetric charge distribution (zero dipole moment), and tries to mold it by a single operation into a giant dipole whose charge is highly focused along the field. On the other hand in multistage shaping one uses one photon to create from a ground state a not too large dipole of charge distribution that is focused along the field at an intermediate state followed by another photon absorption from this intermediate state that produces larger dipole whose charge is even more focused along and so on till one excites the giant dipole in a highly focused distribution along the field.

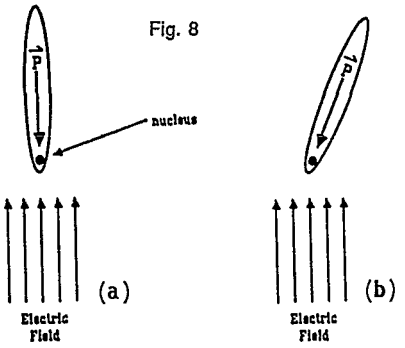

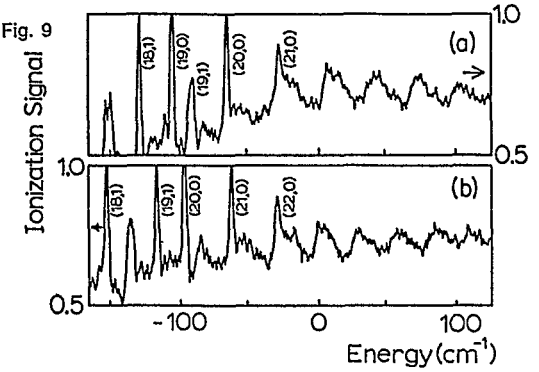

Fig. 8 Schematic of the elliptical orbit (cigar shape) of a giant dipole (a) aligned along the field, and (b) of a giant dipole tilted with respect to the field showing the proton being located near the lower tip.

Fig. 9 The spectrum of hydrogen near E = 0 in the presence of 5 kV/cm (top) and 3 kV/cm (bottom) showing the broad giant dipole states in the positive energy region.

The ability to create moderately large focused dipoles as intermediates is the key to the success of the multistage shaping operation.[28,4,6] This is explained in Fig. 10 for a two-stage process using as an intermediate n = 2 of hydrogen. Because the level splittings in n = 2 of hydrogen are small enough (0.3 cm^{-1}) such that an electric field imposed on the atom which is larger than 5 kV/cm will be able to mix all of these sublevels and hence their charge distributions (each has a zero dipole) to produce distinct dipole distributions needed for the shaping process. Our calculations show that by utilizing the up-field extended dipole of n = 2 as an intermediate, the efficiency can be increased from 10 to 30%, whereas by utilizing the down-field extended dipole the efficiency is reduced to 1%. These were confirmed in our hydrogen experiment as shown in Fig. 11. Our further calculations using higher n states whose charge can be focused along the field more easily, as shown in Fig. 12a, and hence can be matched or tuned more closely to the charge of the giant dipoles, showed dramatic effects on the efficiencies.[28] The use of, for example, n = 9 as the intermediate step in the process, rejects almost completely the excitation of the spectrum of the normal atom in favor of the one-dimensional atom. Results for n = 1, n = 2, and n = 9 are shown in Fig. 12b, along with a schematic of the focusing effect on the intermediates.

The enhanced efficiency is very nice, but it is found that it is practically not possible to increase the lifetime of these giant dipoles in this positive energy region by too much. Such inability is related to the fact that the bound motion of all these giant dipoles in this region are driven by nearly the same charge, most of the nuclear charge $Z_1 \sim 1$, which also dictates very similar orbits where the nucleus is located at the lower tip of the cigar. However, it is found that such enhanced efficiency can be extended to the negative energy region where it is also possible to produce giant dipoles that live quite long. Therefore we will now discuss such promising negative energy regions between E = 0 and $E = E_c$.

In this region the giant dipole atoms take on different properties than the one in the positive energy region. Firstly, the fraction of the charge that drives the bound motion can be varied from 0 to 1 by varying the energy of the system, and consequently the position of the nucleus inside the cigar can also

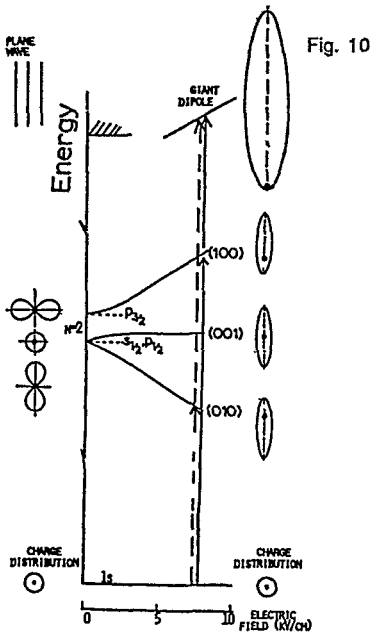

Fig. 10

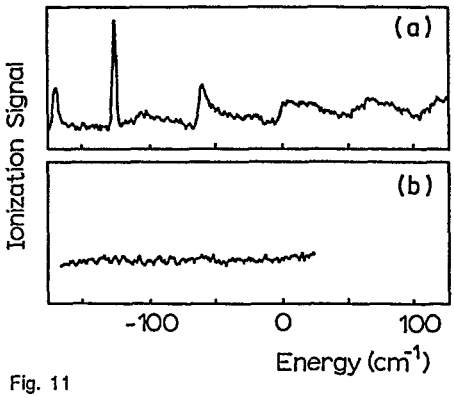

Fig. 11

Fig. 10 Schematic of energy level diagram of hydrogen as a function of the magnitude of the electric field, showing also the charge distribution of the atom at zero field (to the left) and at high fields (to the right). The figure also shows the two stage excitations via the parabolic states of n = 2.

Fig. 11 Absolute experimental spectra in arbitrary units for the two stage process (described in Fig. 10) utilizing the processes shown as solid line (a) and dashed lines (b).

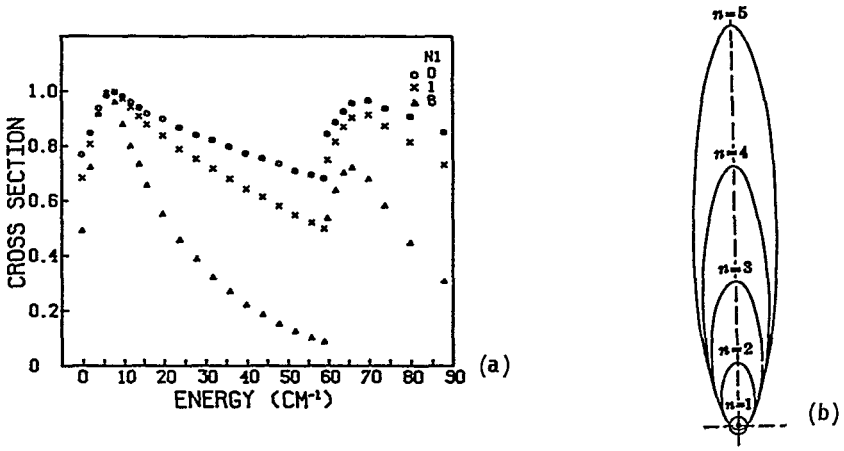

Fig. 12 The two-stage excitation of the giant dipoles utilizing higher states as intermediates. (a) The charge of high n states can be focused along the field more easily and hence can be matched or tuned more closely to the charge of the giant dipoles. (b) Theoretical results for n = 1, n = 2, and n = 9 are shown.

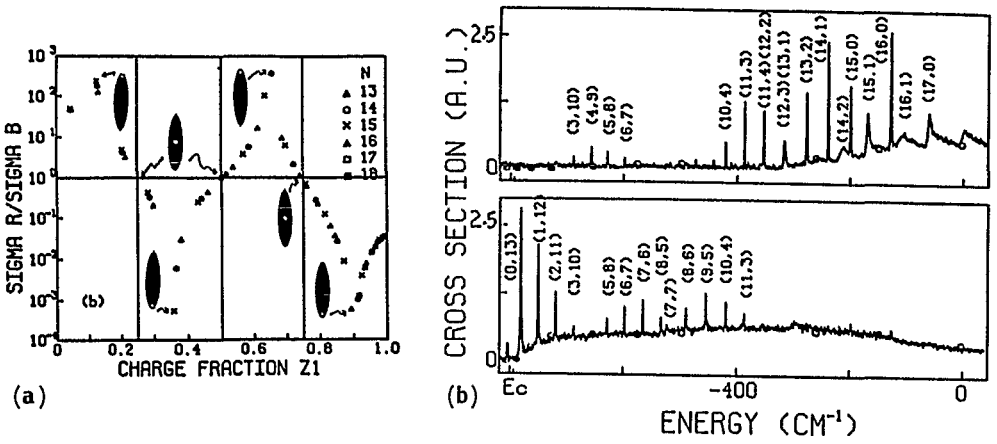

Fig. 13 Long-lived giant dipole atoms in the negative energy region. (a) We plotted an indicator of the location of the nucleus inside the cigar as a function of Z_1 along with sketches of some possible orbits. This indicator is related to the ratio of the area of the orbit below the nucleus to that above the nucleus. (b) The experimental giant dipole spectrum in the negative energy region for the two-stage processes shown of Fig. 10. The top corresponds to the solid line process while the bottom corresponds to the dashed line process of the previous figure.

be controlled. In Fig. 13a we plotted an indicator of the location of the nucleus inside the cigar as a function of Z_1, along with sketches of some possible orbits for the m = 0 case. This indicator is related to the ratio of the area of the orbit below the nucleus to that above the nucleus. The figure shows a remarkable property: for the fractional charges Z_1 = 1/4, 1/2, and 3/4 the nucleus is located at the center of the cigar (the atom has zero dipole moment). These fractional charges thus constitute lines across which the direction of the giant dipole reverses. In the first and third quarters the dipole is along the imposed field whereas in the other two quarters it is opposite to it. Given the size of the orbit (which can be calculated), one can use the above indicator to determine the magnitude of the giant dipole. Moreover, we have recipes to cook up giant dipoles of given Z_1 values. These features and others have been recently confirmed by our experiments. The giant dipole spectrum for m = 0 is shown in Fig. 13.

Figure 14a gives the indicator of the location of the nucleus as a function of Z_1 for the |m| = 1 case. The figure shows that only the fractions 0, 1/2 and 1 are of importance; they give two halves that classify the atoms. Fig. 14b gives the experimental spectrum confirming these results.

Examination of the spectrum indeed shows a variety of widths (lifetimes) that range from quite short to quite long. In fact there are giant dipoles that do not show up in our spectrum because they live longer than the time of measurement, which is 100 ns, or because they radiatively decay before they ionize and hence do not get detected. Again there are systematics to the ionization lifetime as a function of Z_1, and hence as a function of energy, that makes the selection of a giant dipole of given specification possible.

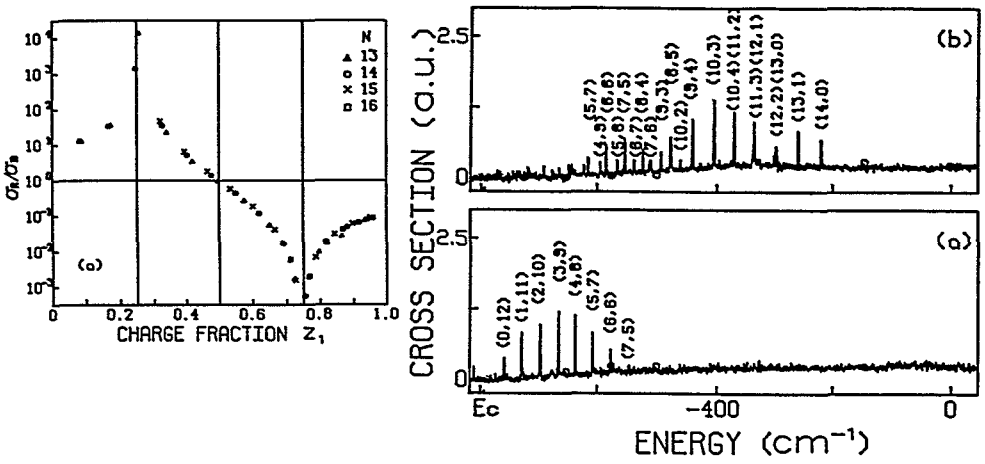

Fig. 14 (a) The indicator of the position of the nucleus, and (b) the hydrogen spectrum for $|m| = 1$ under similar conditions used in the studies given in Fig. 13.

4. Classical Chaos in Microwave Fields

There has been much interest in the question of the existence of chaotic behavior in quantum-mechanical systems whose classical analogues are known to be non-integrable and to exhibit chaotic behavior.[29-38] One system which received much attention theoretically and experimentally is highly excited atomic hydrogen.[29,34,38] We have theoretically analyzed stochasticity in highly excited atomic hydrogen in the presence of a microwave field and a dc electric field using a classical one-dimensional model similar to that of an electron system over a helium surface. We have previously determined in detail the effect of the dc field on the threshold of global stochasticity and on the number of states trapped in the nonlinear resonances.[38]

The basic procedure of our calculation which is based action angle variable has been published before, in general terms[39], for the case without a DC field[3], and for the case of a very high clamping DC field[38,40]. In the presence of strong dc fields, the action angle variables, however, cannot be determined analytically, and thus we did integrals numerically but did not do a numerical simulation. The nonlinear resonance overlap theory we used has proven to be a reliable estimate of the threshold of classical chaos in varying situations.[37,39] For example, the transition to global chaos happens within a factor of about 2 in AC field of the resonance overlap estimate in the problem with no DC field. In Fig. 15 we plot the classical chaos AC field threshold for an electron prepared in a state of given initial action for a number of different DC fields at an AC frequency of 30.5 GHz. For other frequencies all plots in the paper can be scaled; the scaling laws are given in the captions.

There are good theoretical reasons to believe that the number of quantum states trapped in the first nonlinear resonance determines whether the system is in the classical or purely quantum limit, at least in the low-frequency region (below the first resonance.)[41] The system is expected to behave classically when the number of states trapped is >>1, and non-classically when the number of states trapped is $< \approx 1$. With this in mind, we plot in Fig. 16a the number of states trapped in the first

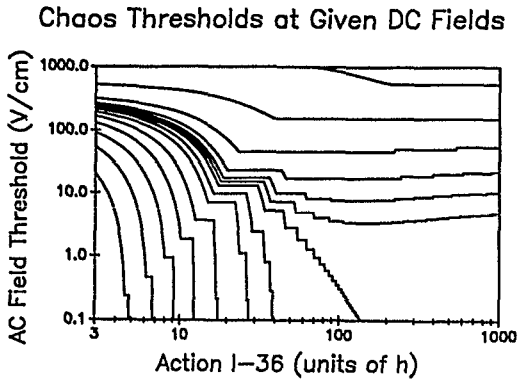

Fig. 15 AC field chaos threshold as a function of the initial action of the system for a number of DC field strengths. These from left to right are: -240, -160, -120, -80, -40, -20, 0, 10, 20, 40, 100, 300, and 1000 V/cm. The frequency of the AC field is 30.5 GHz.

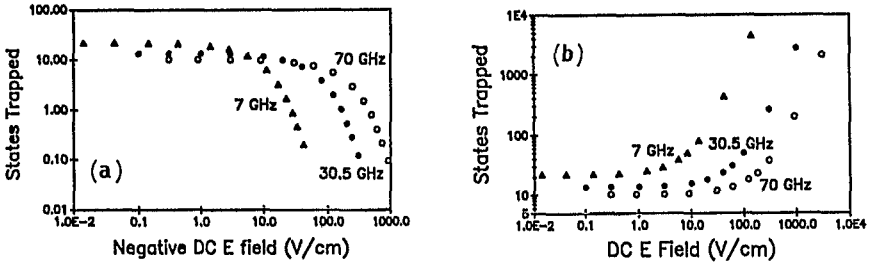

Fig. 16. Number of states trapped in the lowest nonlinear resonance at the threshold of chaos (a) as a function of positive DC E-field, and (b) as a function of negative DC E-field, for a number of frequencies of the AC field: 7GHz, 30.5GHz, and 70GHz.

resonance for a clamping DC field, and in Fig. 16b the same for an unclamping field. These quantities can be read off the Fig. 15 graph; they are simply the widths of the first nonlinear resonances for the different DC fields. The action measured in units of h is equal to the principal quantum number n in the Wilson-Sommerfeld semiclassical theory of quantum mechanics; it is approximately equal for large n in the WKB approximation. Thus, the width of a resonance is a good approximation for the number of states trapped. It is clear that the unclamping field provides a parameter that allows us to go from the classical limit to the uniquely quantum limit. One can see from the graphs that this limit can be reached with easily available microwave frequencies and DC fields. Another advantage of the unclamping DC field is that, by reducing the inherent frequency of the 1D system, it may allow one to more easily reach the regime in which the externally imposed microwave frequency is greater than the inherent system frequency. Uniquely quantum effects which do not occur in the low-frequency regime

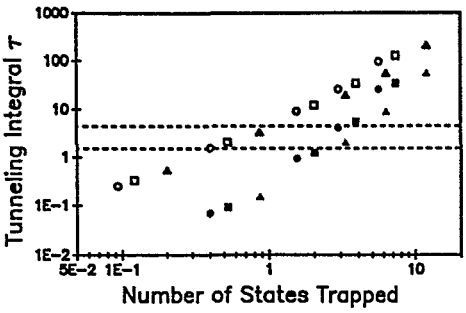

Fig. 17 Tunneling integral τ as a function of the number of state s trapped in the m=1 nonlinear resonance, from the bottom of the m=1 (open symbols) and m=2 (filled symbols) resonances at the threshold of chaos. The triangles are 7 GHz, the squares 30.5 GHz, and the circles 70 GhZ.

have been predicted for this high frequency regime by a quantum-mechanical numerical simulation of the system[42], including the quenching of classical chaos by the quantum system. It appears that the DC field allows one to quickly and easily examine the system for various values of the number of trapped states, down to the quantum regime, and helps one to reach a new regime in the frequency ratio as well. Note that if the hypothesis of the quantum quenching of chaos is true, then the application of the unclamping field, a field trying to rip the electron away from the atom or surface, might actually be a stabilizing factor because it brings the system into the quantum regime.

A question of interest is how few states trapped can be reached without tunneling becoming a problem. With that in mind, we plot in Fig. 17 the tunneling integral τ from states at the bottom and at the top of the m = 1 resonance as a function of the number of states trapped in that resonance at the threshold of chaos. Comparing with tunneling from the initial state, one clearly reaches the quantum regime at τ=1.5, with about 2 states trapped at 30.5 GHz. Note that the number of states trapped at τ=1.5 is fairly insensitive to frequency.

If one is trying to obtain a spectrum, instead of just looking at ionization by chaos, then there is also a maximum τ criterion. For a typical experimental setup (ref. 12), the atom must ionize by tunneling within a microsecond in order to be detected. This criterion gives a maximum τ of about 4.5 for the RIS experiment at 7 GHz (the τ criterion, is slightly larger for the other frequencies plotted). This maximum τ criterion, as well as the minimum, is plotted in Fig. 17. Although the band of observable spectra is fairly narrow in τ, it spans a wide range in the number of states trapped. If one looks at the spectrum low in the first resonance, one can go down to about 0.5 states trapped, and if one looks high in the first resonance, one can see the spectrum for as many as 5 states trapped. Since agreement with classical chaos predictions has been observed for as few as 20 states trapped[43], one might expect 5 states to show at least some classical chaos character. In any case, one could increase the number of states trapped by working at lower frequency. Thus, the spectrum measurement would span the region from the clearly quantum-mechanical to the classical.

5. Frequency Modulation of Hydrogen--Effect of Strong Field on the Dimensionality

The response of hydrogen to strong low frequency radiation has been extensively analyzed classically and quantum mechanically in recent years with the use of a one-dimensional model. In

spite of the extensive use of this model theoretically and experimentally, there is still an uneasy feeling lingering about its validity and applicability in the presence of intense external fields.[42] Although there is some experimental evidence for the preservation of the one-dimensionality during the interaction time, this conclusion was drawn from experiments in which the field was well below the threshold for classical chaos.[34]

We recently examined the effect of the external field on the dimensionality of this system.[19] We attacked this problem by taking some hints from the interaction of polar molecules with intense radiation. Recently it was noted that the existence of a permanent electric dipole in a polar molecule allows absorption of a large number of photons in restricted two level system.[44] These ideas were also extended to the one-dimensional hydrogen atoms.[45] Here we reexamine the interaction and present a view in which the absorption proceeds via single photon absorption by sidebands that are created by the interaction of the intense field with the permanent dipole. In fact the idea of sidebands is not new since Townes reported their existence in his early work on masers. However, this idea has not surfaced in the literature with regard to the recent work of interaction of polar molecules with intense radiation.

Specifically, we analyze the interaction of an intense EM field of amplitude E_0 and frequency ω with a low lying (n in the range of 2 to 9) two level system of "one-dimensional" hydrogen (transition frequency: $\omega_0 \equiv (N+1)\omega$, and transition dipole moment μ).

Since in the presence of the dc field each n state splits into a number of one-dimensional states that are specified by the parabolic quantum numbers n_1, n_2 and m, then there are several transitions within a pair of n manifolds. Ladder transitions are defined by $\Delta n_1 = \Delta n$ for $n_1 \geq n_2$ or by $\Delta n_2 = \Delta n$ for $n_2 \geq n_1$. Off-ladder transitions, on the other hand, are defined by $\Delta n_1 = \Delta n$ for $n_1 \leq n_2$ or by $\Delta n_2 = \Delta n$ for $n_2 \leq n_1$. Finally all other possible transitions will be called "veryoffladder" transitions. Fig. 18 gives the permanent dipole moments for the various states in this range, and the transition dipole moments for some selected transitions. These were calculated using wavefunction of the parabolic states in the zero field limit. Exact numerical calculations indicate that the effect of a field of 3kV/cm on these is no more than a few percent.

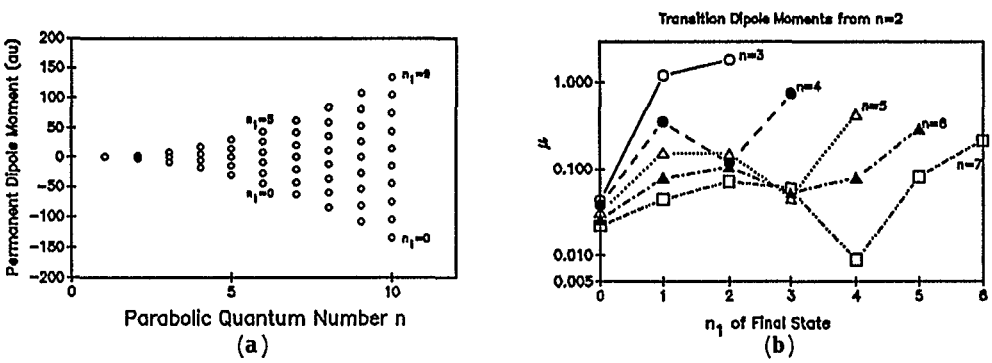

Fig. 18 (a) The permanent dipole moment of the Stark components in the n=2 to n=q manifold calculat ed in the zero field limit. (b) The transition dipole moment to some selected state in $n=3$ to $n=9$ manifold from the bluest component of n=2 (1,0,0).

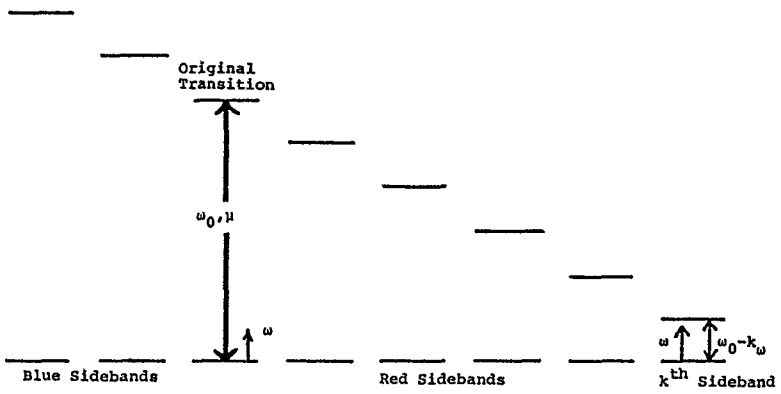

Fig. 19 A schematic of the energy diagram of the field induced sidebands of a given one-dimensional two level system, showing semi-infinite red and blue bands.

The interaction can be outlined as follows. The field couples strongly to the permanent dipole moments of the two levels (d_1 and d_2), frequently modulating the system and hence creating a large number of equally spaced sidebands (spacing equal to ω that share μ among themselves). This is shown schematically in Fig. 19 for illustration. The distribution of μ_n depends on $(d_2-d_1)E_0/\omega$. Figure 20 shows, as an example, the oscillator strength distribution for the transition between the two extreme blue states (ladder transition) of n=2 and n=3 manifolds, namely (1,0,0) and 2,0,0). The rest of the infinite number of the sidebands are not shown because their oscillator strength is very negligible and will not affect the effective band width of the modulation.

Because the N^{th} sideband where $(N+\omega)\omega\cong\omega_0$ is the only sideband which is in near single photon resonance, it will dominate the interaction especially at high enough intensities where its fraction of the transition dipole moment is sizeable. We determined the transition moment of the N^{th} sideband for a variety of ladder, offladder and veryoffladder systems. Our results, an example of which is shown in

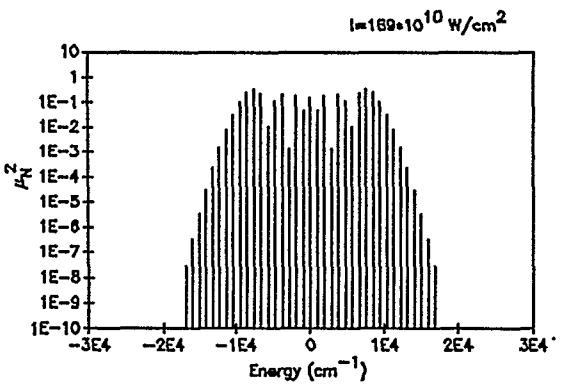

Fig. 20 The square of the induced oscillator strengths of the sidebands ot a two level system of the bluest components of n=2 and n=3 of hydrogen: 1,0,0 and 2,0,0 respectively. The weak bands are not shown and they will not affect the effective bandwidth of the system.

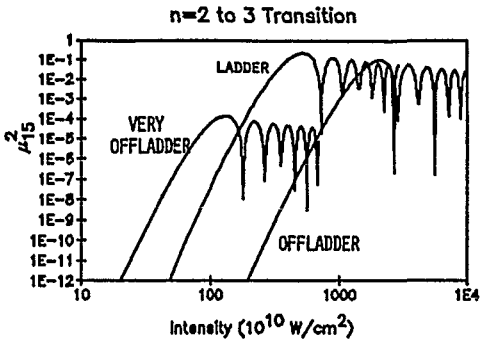

Fig. 21 The oscillator strength of the 15th side band of three transitions all originating from 1,0,0, the bluest component of n=2 as a function of the intensity of the 10.6μ radiation. The ladder transition is to (2,0,0), and off ladder is to (1,1,0), and the very off ladder is to (0,2,0) of the n=3 manifold. The local minima shown are actually zeroes. They are not plotted as such because only a finite number of points are plotted, and to improve the graph's readability.

Fig. 21, indicate that the veryoffladder transitions are very weak at all intensities. However at sufficiently high intensities, offladder sidebands may become as strong as ladder sidebands, thus breaking the one-dimensionality of the system. It is interesting to note that this loss of one-dimensionality occurs at powers close to those needed to induce global classical chaos of the system (this threshold marked on the figure). The onset of classical chaos was calculated using a one dimensional classical model similar to that of an electron near a helium surface as described in the previous section.

The calculations also show that the intensity I_b needed to break the dimensionality for transition in the n and n+1 manifold drops as n increases. These are shown in Fig. 22. It is interesting to plot, for

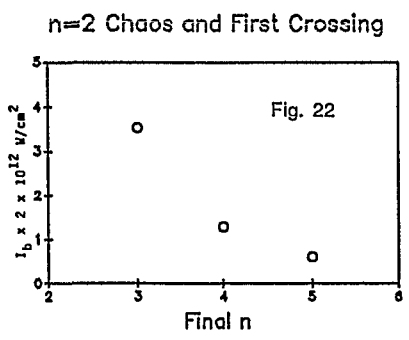

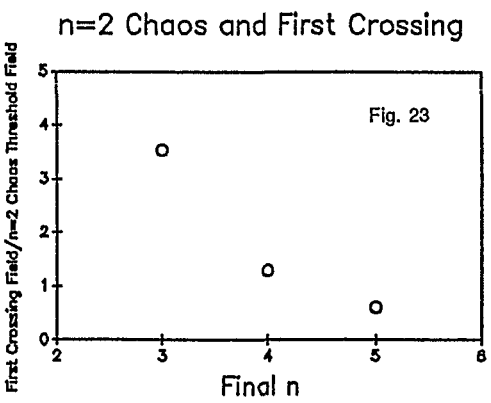

Fig. 22 The intensity of the ac field needed to break the one dimensionality of transition between n-1 and n manifolds, i.e. the intensity at which ladder and off ladder transitions become of equal strength.

Fig. 23 The one-dimensionality window, i.e. the ratio of the intensity needed to break the one-dimensionality of transition between n-1 and n where n=2, 3,. . . to the chaos threshold of n_0=2, as a function of n.

a given initial manifold, n_0, the ratio $R = I_b/I_c$ as a function of n where I_c is the intensity at which the initial state gets into the chaos regime. This ratio or what we call window is useful in the discussion of dimensionality of a chaotic system. As an example we plot in Fig. 23 the window for a system that is initially prepared in (1,0,0) of n=2 of hydrogen for which the classical chaos threshold at 10.6μ is $1.7 \times 10^{12} W/cm^2$. The figure shows that the window closes ($R \cong 1$) as the excitation reaches n = 5. It is to be noted that the interaction of 10.6μ radiation with the transition between n=6and n=7 manifold falls in the high frequency regime, i.e. $\omega \geq \omega_0$

We also studied the frequency dependence of these results. Using radiation of 21.2μ, we find that the intensity at which the offladder and ladder strengths become comparable does not change. This is reasonable since the order of the Bessel function as well as its argument depend on the frequency in manner that causes cancellation of the overall dependence. For instance $(\kappa + 1)$ is proportional to $\frac{1}{\omega}$ where κ is the order of the Bessel function, and the Bessel function of order κ peaks at $\Delta dE/\omega$ which is proportional to $(\kappa+1)$. Thus the magnitude of E at which the offladder transition becomes just as strong as the ladder transition is essentially frequency independent.

The chaos threshold, on the other hand, depends on the frequency. However, at sufficiently low frequencies such as the ones being used here, the chaos threshold is expected to be somewhat insensitive to frequency, since the conditions are close to the dc limit.[37] Thus one expects the window R to be nearly frequency independent. Numerical results for the case of 21.2μ are shown on Fig. 23 which also displays the 10.6μ case, showing the frequency independence.

Finally the condition of high/low frequency, on the other hand, depends strongly on the frequency, and therefore it is possible to conceive situations such that as the ionization proceeds, the system loses one-dimensionality before the high frequency regime is reached.

6. Conclusion

The last few years have seen a lot of progress in the deliberate manipulation of atomic structure by imposing strong external fields. These include other than electric fields such as dc magnetic fields which were shown to allow construction of two-dimensional atoms. For example, we can now design and construct atoms which are effectively one dimensional. The main directions we perceive for future work are: First, further development and understanding of the potentiality for and constraints on effective manipulation. Second, elucidation of the ways in which these new species of atoms interact with the physical and chemical environment. And third, we will see their utilization in scientific and technological applications, especially those which take advantage of the lower dimensionality which makes complex problems more amenable to theoretical treatment and interpretation. One example, mentioned above, is the study of chaotic dynamics in nonintegrable systems, a subject that is encountered in research areas as diverse as classical mechanics, chemical reaction, and quantum mechanics.

REFERENCES

[1] R. R. Freeman, N. P. Economou, G. C. Bjorklund, and K. T. Lu, Phys. Rev. Lett. 41, 1463 (1978).

[2] C. W. Clark, K. T. Lu, and A. F. Starce, in Progress in Atomic Spectroscopy, eds. H. Beyer and H. Kleinpoppen (Plenum, New York, 1984).

[3] See articles in Atomic Excitation and Recombination in External Fields, ed. M. H. Nayfeh and C. W. Clark (Gordon and Breach, New York 1985).

[4] U. Fano, Colloq. Int. CNRS 273, 127 (1977); Phys. Rev. A 24, 619 (1981).

[5] M. H. Nayfeh, K. Ng. and D. Yao in SEICOLS, Laser Spectroscopy, T. Hänsch and R. Shen, eds. (Springer-Verlag, Berlin, Heidelberg, 1985). p. 71.

[6] M. H. Nayfeh, D. Yao, Y. Ying, D. Humm, K. Ng and T. Sherlock: In Advances in Laser Science - 1, AIP Conference Proceedings 146, 370 (1986).; M. H. Nayfeh, in Resonance Ionization Spectrocopy, U. K. Institute of Physics, Number 84, G. S. Hurst and C. G. Morgan, eds., 21 (1986); M. H. Nayfeh in Lasers, Spectroscopy and New Ideas, W. Yen and M. Levenson, eds. (Springer-Verlag, Berlin, 1987), p. 141.

[7] T. S. Luk, L. DiMauro, T. Bergeman, and H. Metcalf, Phys. Rev. Lett. 47, 83 (1981).

[8] S. Feneuille, S. Liberman, E. Luc-Koenig, J. Pinard, and A. Taleb, Phys. Rev. A 25, 2853 (1982).

[9] W. Sandner, K. A. Safinya, and T. F. Gallagher, Phys. Rev. A 23, 2448 (1981).

[10] W. Glab, G. B. Hillard, and M. H. Nayfeh, Phys. Rev. A 28, 3682 (1983).

[11] K. H. Welge and H. Rottke, in Laser Techniques in the Extreme Ultraviolet-OSA, Boulder, Colorado, 1984, edited by S. E. Harris and T. B. Lucatorto, AIP Conf. Proc. No. 119 (AIP, New York, 1984), pp. 213-219.
H. Rottke and K. H. Welge, Phys. Rev. A 33, 301 (1986).

[12] W. L. Glab and M. H. Nayfeh, Phys. Rev. A 31, 530 (1985).

[13] E. Luc-Koenig and A. Bachelier, Phys. Rev. Lett. 43, 921 (1979).

[14] A.R.P. Rau and K. T. Lu, Phys. Rev. A 21, 1057 (1980).

[15] D. A. Harmin, Phys. Rev. A 24, 2491 (1981); D. A. Harmin, Phys. Rev. Lett. 49, 128 (1982); Phys. Rev. A 26, 2656 (1982).

[16] W. D. Kondratovich and V. N. Ostrovsky, Zh. Eksp. Teor. Fiz. 4, 1256 (1982).

[17] K. Ng, D. Yao and M. H. Nayfeh, Phys. Rev. A 35, 2508 (1987).

[18] D. Yao, K. Ng, M.H. Nayfeh, Phys. Rev. A. (Dec.) 1987.

[19] M. H. Nayfeh, Bulletin Am. Phys. Soc., March (1988).

[20] J. E. Bayfield, L. D. Gardner, and P. M. Koch: Phys. Rev. Lett. 39, 76 (1977);
P. M. Koch: Phys. Rev. Lett. 41, 99 (1978).

[21] H. C. Bryant et al. Phys. Rev. A 27, 2889, 2912 (1983); W. W. Smith et al. in Atomic Excitation and Recombination in External Fields, M. H. Nayfeh, and C. Clark eds., (Gordon and Breach, New York, 1985).

[22] G. C. Bjorklund, R. R. Freeman, and R. H. Storz, Opt. Comm. 31, 47 (1979).

[23] W. L. Glab and M. H. Nayfeh, Opt. Lett. 8, 30 (1983); W. Glab, Ph.D Thesis, University of Illinois, 1984 (unpublished).

[24] M. H. Nayfeh, K. Ng, and D. Yao in Atomic Excitation and Recombination in External Fields, M. H. Nayfeh and C. W. Clark eds., (Gordon and Breach, New York, 1985).
[25] T. W. Hänsch, S. A. Lee, R. Wallenstein, and C. Wieman, Phys. Rev. Lett., 34, 307 (1975).
[26] W. L. Glab, K. Ng, D. Yao, and M. H. Nayfeh, Phys. Rev. A 31, 3677 (1985).
[27] G. Luders, Ann. d. Phys. [6], 8, 301 (1951).
[28] Y. Ying and M. H. Nayfeh, Phys. Rev. A 35, 1945 (1987).
[29] G. Casati, B. V. Chirikov, F. M. Israelev, J. Ford: In Stochastic Behavior in Classical and Quantum Systems, ed. by G. Casati and J. Ford, **Lecture Notes in Physics**, Vol. 93, (Springer, New York, 1979).
[30] D. R. Grempel, S. Fishman, and R. E. Prange: Phys. Rev. Lett. 49, 833 (1982).
[31] M. V. Berry: Physica (Amsterdam) 10D, 369 (1984).
[32] S. J. Chang and K. J. Shi: Phys. Rev. Lett. 55, 269 (1985).
[33] E. V. Shuryak: Zh. Eksp. Teor. Fiz. 71, 2939 (1975); Sov. Phys. JETP 44, 1070 (1976); P. I. Belobrov, G. P. Berman, G. M. Zaslavski, and A. P. Slivinskii: ibid. 76, 1960 (1979); 49, 993 (1979).
[34] J. E. Bayfield and L. A. Pinnaduwage: Phys. Rev. Lett. 54, 313 (1985).
[35] P. M. Koch: J. Phys. (Paris), Colloq. 43, C2-187 (1982).
[36] D. Humm and M. H. Nayfeh: to be published.
[37] R. V. Jensen: Phys. Rev. A 30, 386 (1984); in Chaotic Behavior in Quantum Systems, ed. by G. Casati, (Plenum, London 1985).
[38] M. H. Nayfeh and D. Humm in Proceedings of the International Workshop on Photons and Continuum States, ed. by N. Rahman, (Cortona, Italy 1986), (Springer, Berlin, Heidelberg 1987).
[39] B. V. Chirikov, Phys. Rep. 52, 549 (1979); G. M. Zaslavsky and B. V. Chirikov, Usp. Fiz. Nauk. 105, 3(1971) [Sov. Phys. Usp. 14, 263(1971).
[40] G. P. Berman, G. M. Zaslavsky, and A. R. Kolovsky, Zh. Elesp. Teor. Fiz. 88, 1551(1985) [Sov. Phys. JETP G1, 925 (1985)].
[41] G. P. Berman, G. M. Zaslavsky, and A. R. Kolovsky, Phys. Lett. 87A, 152 (1982).
[42] G. Casati, B. Chirikov, D. Shepelyansky, and I. Guarneri, Phys. Rep. 154, 29 (1987).
[43] R. V. Jensen and S. M. Susskind, in Photons and Continuum States of Atoms and Molecules, eds. N. Rahman, C. Guidotti and M. Allegrini, 13 (Springer-Verlag 1987).
[44] W. J. Meath and E. A. Power, Canadian Molecular Phys. 51, 585 (1984).
[45] J. E. Bayfield, in Photons and Continuum States of Atoms and Molecules, eds. N. Rahman, C. Guidotti, and M. Allegrini, (Springer-Verlag) 8, 1987.